Comparison of Entropy Production Rate Minimization Methods for Binary Diabatic Distillation

ARTICLE · OCTOBER 2002

CITATIONS
23

READS
24

2 AUTHORS:

Gelein M de Koeijer
Statoil ASA
27 PUBLICATIONS **603** CITATIONS
SEE PROFILE

Signe Kjelstrup
Norwegian University of Science and Techno…
316 PUBLICATIONS **3,719** CITATIONS
SEE PROFILE

Comparison of Entropy Production Rate Minimization Methods for Binary Diabatic Distillation

Gelein M. de Koeijer* and Signe Kjelstrup

Department of Chemistry, Norwegian University of Science and Technology, Sem Sælands vei 14, N-7491 Trondheim, Norway

Peter Salamon and Gino Siragusa

Department of Mathematical Sciences, San Diego State University, San Diego, California 92182-7720

Markus Schaller and Karl Heinz Hoffmann

Institute of Physics, Chemnitz University of Technology, D-09107 Chemnitz, Germany

The purpose of this study is to compare two analytical methods with two numerical methods for minimizing the entropy production rate in diabatic distillation columns (i.e., with heat exchangers on all trays). The first analytical method is the equal thermodynamic distance method. The second uses Lagrange minimization on a model derived from irreversible thermodynamics. The numerical methods use Powell's and a Monte Carlo algorithm and gave the same results. Both analytical methods agreed well with the numerical ones for two columns with low separation per tray, while they did not agree well for a column with large separation per tray.

1. Introduction

This work is inspired by Andresen and Salamon[1] and De Koeijer and Kjelstrup,[2] in which minimization of the entropy production rate of diabatic distillation is discussed. Diabatic distillation columns have heat exchangers on all trays. They are known[3−8] to have a better second law efficiency than adiabatic distillation columns with only two heat exchangers: the reboiler and the condenser. Besides giving a more prudent use of energy, there are indications that diabatic distillation is also economically feasible.[9,10] Despite these advantages, diabatic distillation is still relatively unexplored. No design method is established, and there is only one systematic experimental study by Rivero.[5]

The central question is how to obtain maximum second law efficiency or minimum entropy production rate by distributing the heating and cooling capacity over the column, i.e., how to obtain the best duty profile. The design of the column will depend on these results. In recent years four different methods have been published on how to determine the duty profile. Among these four methods, two are analytical and two are numerical. One analytical method was described by Andresen and Salamon.[1] It is called the principle of equal thermodynamic distance (ETD) and uses the thermodynamic geometry of the system in state space. De Koeijer and Kjelstrup[2] presented another analytical method together with a numerical method. The analytical method applied Lagrange minimization and irreversible thermodynamics. The numerical method is based on a Monte Carlo algorithm. A second numerical method applies Powell's algorithm[11] to a normal entropy balance.[12] All four methods minimize the entropy production rate due to heat and mass transfer on the trays only.

* To whom all correspondence should be addressed. Present address: Statoil ASA, Corporate Strategic Technology, Arkitekt Ebbellsvei 10, N-7005 Trondheim, Norway. Tel: +47 73584011. Fax: +47 73967286. E-mail: gdek@statoil.com.

Table 1. Column Characteristics

	column		
	A	B	C
no. of trays	20	20	70
x_b^B	0.10	0.01	0.01
x_b^D	0.90	0.99	0.99

The occurrence of four different methods for one problem created a discussion on the predictive power, accuracy, and applicability of those methods. The purpose of this work is to compare these four methods for three example columns. Furthermore, the difference between adiabatic and diabatic columns will be discussed.

We shall see that the numerical methods agree essentially over the whole range of variations. This means that such methods can be used as benchmarks for the analytical methods, and we shall therefore do this. The two analytical methods have different characteristics and do not always follow the results of the numerical methods. The purpose of analytical methods is to give physical insight.

2. The System

The system is a diabatic distillation column, i.e., with heat exchangers on all trays. We use three columns that all separate benzene and toluene. The feed is always $F = 1.00$ mol/s with a feed mole fraction of benzene, $x_b^F = 0.5$. Table 1 gives the parameters that differ between the three columns.

The most realistic column is column B. Column C has an unreasonable number of trays, while column A has a rather low purity of the products. Physical chemical properties of the binary mixture are given in Table 2.

Tray characteristics are calculated by a top-to-bottom tray-to-tray calculation with the assumption that equilibrium is established on each tray using eqs 1−3.

10.1021/ie010872p CCC: $22.00
Published on Web 10/16/2002

Table 2. Physical Chemical Properties

	benzene	toluene
T^{boil} (K)	353.25	383.78
$C_{\mathrm{p}}^{\mathrm{vap}}$ (J/mol·K)	81.63	106.01
$C_{\mathrm{p}}^{\mathrm{liq}}$ (J/mol·K)	133.50	156.95
$\Delta_{\mathrm{vap}}H(T^{\mathrm{boil}})$ (J/mol)	33 600	38 000
S_0^{liq} (J/mol·K)	269.20	319.74

Further assumptions are temperature-independent heat capacities for both phases and a constant pressure (10^5 Pa). The feed and products are taken to be liquids at their boiling points. The assumption of equimolar overflow is not used because an incorrect enthalpy balance leads to an incorrect entropy balance. Equilibrium mole fractions for each tray were determined from an integrated form of the Clausius−Clapeyron equation for a regular solution.[13]

$$y_{\mathrm{b},n} = x_{\mathrm{b},n}\exp\left[\frac{\omega}{RT_n}(1-x_{\mathrm{b},n})^2\right]\times \exp\left[\frac{\Delta_{\mathrm{vap}}H_{\mathrm{b}}(T)}{R}\left(\frac{1}{T_{\mathrm{b}}^{\mathrm{boil}}}-\frac{1}{T_n}\right)\right]$$

$$1-y_{\mathrm{b},n} = (1-x_{\mathrm{b},n})\exp\left[\frac{\omega}{RT_n}x_{\mathrm{b},n}{}^2\right]\times \exp\left[\frac{\Delta_{\mathrm{vap}}H_{\mathrm{t}}(T)}{R}\left(\frac{1}{T_{\mathrm{t}}^{\mathrm{boil}}}-\frac{1}{T_n}\right)\right] \quad (1)$$

The nonideality parameter ω is 252.50. For each tray number n, a specified temperature T_n in eq 1 determines the corresponding pair of mole fractions in the gas ($y_{\mathrm{b},n}$) and the liquid ($x_{\mathrm{b},n}$). The mass balances are used to calculate the mass flows (L_n and V_n) on each tray.

$$V_n + L_n = V_{n+1} + L_{n-1}$$

$$V_n y_{i,n} + L_n x_{i,n} = V_{n+1}y_{i,n+1} + L_{n-1}x_{i,n-1} \quad (2)$$

The duties of the heat exchangers are calculated from the energy balance over the tray.

$$V_n H_n^{\mathrm{V}} + L_n H_n^{\mathrm{L}} = V_{n+1}H_{n+1}^{\mathrm{V}} + L_{n-1}H_{n-1}^{\mathrm{L}} + Q_n \quad (3)$$

The entropy production rate on the tray is then given by

$$\left[\frac{\mathrm{d}S^{\mathrm{irr}}}{\mathrm{d}t}\right]_n = V_n S_n^{\mathrm{V}} + L_n S_n^{\mathrm{L}} - Q_n/T_n - V_{n+1}S_{n+1}^{\mathrm{V}} - L_{n-1}S_{n-1}^{\mathrm{L}} \quad (4)$$

The feed tray is located on the tray where the liquid mole fraction of benzene becomes lower than the feed mole fraction. From the mass and energy balances on the tray, the total entropy production rate of the whole column is obtained as

$$\frac{\mathrm{d}S^{\mathrm{irr}}}{\mathrm{d}t} = BS^{\mathrm{B}} + DS^{\mathrm{D}} - FS^{\mathrm{F}} - \sum_{n=0}^{N}\frac{Q_n}{T_n} \quad (5)$$

This is the objective function for the ETD method as well as the two numerical methods. Q_0 is the duty of the heat exchanger that condenses vapor flow V_1 totally, i.e., the condenser.

Alternatively, the objective function can also be set up from knowledge of the transport processes on each tray, using irreversible thermodynamics.[14] The entropy production rate of tray n is

$$\left[\frac{\mathrm{d}S^{\mathrm{irr}}}{\mathrm{d}t}\right]_n = J_{\mathrm{q},n}X_{\mathrm{q},n} + J_{\mathrm{b},n}X_{\mathrm{b},n} + J_{\mathrm{t},n}X_{\mathrm{t},n} \quad (6)$$

$J_{\mathrm{q},n}$ is the flow of heat, $J_{\mathrm{b},n}$ and $J_{\mathrm{t},n}$ are flows of benzene and toluene across the phase boundary, and $X_{\mathrm{q},n}$, $X_{\mathrm{b},n}$, and $X_{\mathrm{t},n}$ are the conjugate driving forces. The objective function is now obtained by summing over all trays. Entropy production in the heat exchangers that supply Q_n is not included in either of the objective functions. The adiabatic column is also simulated with the tray-to-tray method where Q_2, ..., Q_{N-1} are zero. This means that Q_0 and Q_1 form together the condenser and Q_N is the reboiler.

3. Powell's Method

Powell's algorithm is a multidimensional optimization routine. The entropy production rate, expressed by eq 5, is minimized, and the corresponding temperature for each tray is determined. Because the temperature T_1 at the top tray and the temperature T_N at the reboiler are fixed by the given distillate and bottom purity requirements $x_{\mathrm{b}}^{\mathrm{D}}$ and $x_{\mathrm{b}}^{\mathrm{B}}$, the number of control variables is $M = N - 2$. As initial guesses $\tilde{\mathbf{T}}_0$ of temperatures on the trays, we used linear temperature profiles. The following procedure was repeated until the entropy production rate stopped decreasing. For each search direction $\tilde{\mathbf{u}}_j$, $j = 1, ..., M$, the entropy production rate is minimized along that direction, using the temperature profile $\tilde{\mathbf{T}}_{j-1}$ as starting point. The result of this minimization is saved as $\tilde{\mathbf{T}}_j$. The line minimization is performed by a bracketing routine and parabolic interpolation (Brent's method). The direction along which the entropy production made its largest decrease Σ is named $\tilde{\mathbf{u}}_\Sigma$ and saved along with the net displacement $\tilde{\mathbf{T}}_M - \tilde{\mathbf{T}}_0$. When the temperature dependence of the entropy production rate from eq 5 is written as $\mathrm{d}S^{\mathrm{irr}}/\mathrm{d}t(\tilde{\mathbf{T}})$, the following quantities are introduced:

$$\xi_0 \equiv \frac{\mathrm{d}S^{\mathrm{irr}}}{\mathrm{d}t}(\tilde{\mathbf{T}}_0) \qquad \xi_{\mathrm{M}} \equiv \frac{\mathrm{d}S^{\mathrm{irr}}}{\mathrm{d}t}(\tilde{\mathbf{T}}_{\mathrm{M}})$$

$$\xi_{\mathrm{E}} \equiv \frac{\mathrm{d}S^{\mathrm{irr}}}{\mathrm{d}t}(2\tilde{\mathbf{T}}_M - \tilde{\mathbf{T}}_0) \quad (7)$$

If at least one of the inequalities

$$\xi_{\mathrm{E}} \geq \xi_0 \quad (8)$$

or

$$\frac{2(\xi_0 - 2\xi_{\mathrm{M}} + \xi_{\mathrm{E}})[(\xi_0 - \xi_{\mathrm{M}}) - \Sigma]}{\Sigma(\xi_0 - \xi_{\mathrm{E}})^2} \geq 1 \quad (9)$$

holds, then the old search direction set is kept, $\tilde{\mathbf{T}}_M$ is saved as $\tilde{\mathbf{T}}_0$, and the program returns to do another iteration of the algorithm. If the inequalities do not hold, the direction of largest decrease $\tilde{\mathbf{u}}_\Sigma$ is discarded and $\tilde{\mathbf{u}}_M$ is assigned to $\tilde{\mathbf{u}}_\Sigma$. This avoids a buildup of linear dependence of the search directions. $\tilde{\mathbf{T}}_M - \tilde{\mathbf{T}}_0$ is assigned to $\tilde{\mathbf{u}}_M$. A line minimization is done along the new $\tilde{\mathbf{u}}_M$,

and the result is saved as $\tilde{\mathbf{T}}_0$. The algorithm is repeated until the required accuracy is achieved.

4. Monte Carlo Method

The method was in essence presented by De Koeijer and Kjelstrup.[2] The Monte Carlo algorithm starts from either a linear temperature profile or a temperature profile of the adiabatic column. It changes on a random tray the temperature with a random step that is multiplied with a factor *f*. If the entropy production rate of the new profile is larger or if the profile is not physically realizable, the profile is rejected, and a new random step is tried on the previous profile. If the entropy production rate is lower, the new profile is accepted as a new starting point for a new random step on a random tray. This procedure is repeated 2000 times. Then the factor *f* is decreased, and the procedure is repeated again. The factor *f* decreases exponentially in seven steps. When the factor *f* reaches its lowest value, the resulting minimum is recorded. To test whether this minimum can be lowered, the temperature on one random tray is changed; i.e., the temperature profile is perturbed. The whole procedure is repeated again up to 1000 times. If there is no change in the course of 1 day, the procedure is stopped and a minimum is obtained.

5. ETD

Thermodynamic distance measures the length of a path in the set of equilibrium states of a thermodynamic system. The system of relevance for the present discussion is a two-phase binary mixture. An equilibrium state of this mixture is specified once we are given the temperature and the number of moles of liquid and vapor. The path of interest is defined using the temperature T as the parameter, where $L(T)$ and $V(T)$ are obtained by solving the mass balance conditions corresponding to the limit of an infinite number of trays to give

$$V(T) = \frac{x_D - x(T)}{y(T) - x(T)} D \tag{10}$$

$$L(T) = \frac{x_D - y(T)}{y(T) - x(T)} D \tag{11}$$

above the feed and

$$V(T) = \frac{x(T) - x_B}{y(T) - x(T)} B \tag{12}$$

$$L(T) = \frac{y(T) - x_B}{y(T) - x(T)} B \tag{13}$$

below the feed. The discontinuity at the feed is handled by an isothermal path along which the quantities L and V change linearly. It makes no difference how we move across this portion of the path. As long as we keep the temperature constant, this portion of the path is associated with zero length and zero dissipation.[15]

According to the principle of ETD,[1,15,16] the optimal way to traverse this path using a sequence of N equilibrations is in equidistant stages, i.e., such that the distance along that path between the nth and the $(n + 1)$th tray be the same for all n. In general, distance is measured by using the second derivative of the entropy of the system with respect to the extensive variables as a Riemannian metric.[17] In this particular case, this reduces to a simpler expression, with the infinitesimal length $\mathrm{d}\mathscr{L}$ being given by

$$\mathrm{d}\mathscr{L} = \sqrt{\sum_{i,j} \frac{\partial^2 S}{\partial Z_i \partial Z_j} \mathrm{d}Z_i \, \mathrm{d}Z_j} = \frac{\sqrt{C_\sigma}}{T} \mathrm{d}T \tag{14}$$

where the Z_i values are the extensive variables of the system and C_σ is the constant-pressure coexistence heat capacity,[1,15] i.e., the heat capacity that a sample consisting of $L(T)$ moles of liquid and $V(T)$ moles of vapor has while the two phases coexist at constant pressure. To establish an ETD path from the condenser T_0 to the reboiler T_N in a column with N trays, one has to determine temperatures T_n such that

$$\int_{T_n}^{T_{n+1}} \frac{\sqrt{C_\sigma}}{T} \mathrm{d}T = \frac{1}{N} \int_{T_0}^{T_N} \frac{\sqrt{C_\sigma}}{T} \mathrm{d}T, \quad n = 0, \ldots, N - 1 \tag{15}$$

The ETD principle is derived by approximating the entropy production rate to lowest nonzero order in $1/N$. For a small equilibration, the entropy production rate is quadratic to lowest order, and this quadratic part is (by definition) the square of the length element. Minimizing the sum of the squares of the lengths with the constraint of constant total length yields the ETD principle. The sequence of temperatures obtained is then used as the temperature profile for the calculation of column parameters as described in the previous section. Note that the mass flow rates L_n and V_n obtained in this fashion do not lie on the curve $L(T)-V(T)$ used for the determination of the temperature profile, although they do fall close to the curve and approach it as $N \to \infty$. The entropy production rate obtained by this procedure turns out to match the optimal entropy production to third order in $1/N$.[18]

A known limitation of the ETD method is the requirement for a minimum column length. This limitation is due to the fact that the tray−tray separation cannot get too large. In particular,

$$x_{n-1} \leq y_n \tag{16}$$

is a fundamental physical constraint on how far apart two adjacent trays in a distillation column can be. For a certain total length $\mathscr{L}$ and number of trays N, each ETD step must go a distance $\mathscr{L}/N$. For sufficiently large N, condition (16) is never a problem. The condition typically becomes a problem already for column lengths of about 50% longer than conventional lengths.

6. Lagrange Minimization with Irreversible Thermodynamics

The three fluxes and forces of heat and mass transport that are given in eq 6 cannot be calculated without knowledge of the transport processes. In distillation, these transport processes vary across the phase boundary of one tray n, and some average and integration procedures are needed. When one uses the assumption of equilibrium between gas and liquid at the outlet of a tray, integrated fluxes and average forces can be defined.[2,19] Next it is assumed that the entropy production rate stems from the gas side of the phase boundary and that there is a negligible contribution from the

thermal force.[20] The driving forces are then related via the Gibbs−Duhem equation. The approximate entropy production rate of a column is

$$\sum_{n=1}^{N}\left[\frac{dS_{irr}}{dt}\right]_n = \sum_{n=1}^{N}(J_{b,n}X_{b,n} + J_{t,n}X_{t,n}) = \sum_{n=1}^{N}(J_{b,n} - \bar{y}_n J_{t,n})X_{b,n} \quad (17)$$

where $J_{b,n}$ and $J_{t,n}$ are flows of benzene and toluene across the phase boundary in mol/s, $X_{b,n}$ and $X_{t,n}$ are the corresponding driving forces, and $\bar{y}_n$ is the average mole fraction ratio in the Gibbs−Duhem equation. On tray number n, the average driving force for benzene is

$$X_{b,n} = R\ln(y_{b,n}/y_{b,n+1}) \quad (18)$$

It was shown[2] that this model was a good approximation to eq 4 for two columns. The sum of the contributions from all trays is minimized with the Lagrange method as follows:

$$\text{minimize} \sum_{n=1}^{N}\left[\frac{dS^{irr}}{dt}\right]_n = \sum_{n=1}^{N}(\ell_{b,n} - \bar{y}_n\ell_{t,n})X_{b,n}^2 \quad (19)$$

subject to

$$R\ln(x_b^D/x_b^B) = \sum_{n=1}^{N}X_{b,n} = I_1$$

$$R\ln(x_t^D/x_t^B) = \sum_{n=1}^{N}X_{t,n} = I_2$$

$$Fx_b^F - Bx_b^B = \sum_{n=1}^{N}J_{b,n} = I_3$$

$$Fx_t^F - Bx_t^B = \sum_{n=1}^{N}J_{t,n} = I_4 \quad (20)$$

The four constraints in eq 20 ensure that the production level and the purity of products are as required. The solution has the following structure:

$$\begin{bmatrix} 1 & 1 & . & 1 \\ -\bar{y}_1 & -\bar{y}_2 & . & -\bar{y}_N \\ \ell_{b,1} & \ell_{b,2} & . & \ell_{b,N} \\ \ell_{t,1} & \ell_{t,2} & . & \ell_{b,N} \end{bmatrix}\begin{bmatrix} X_{b,1} \\ X_{b,2} \\ . \\ . \\ X_{b,N} \end{bmatrix} = \begin{bmatrix} I_1 \\ I_2 \\ I_3 \\ I_4 \end{bmatrix} \quad (21)$$

$$\begin{bmatrix} -\ell_{b,1} & -\ell_{t,1} & -1 & \bar{y}_1 \\ -\ell_{b,2} & -\ell_{t,2} & -1 & \bar{y}_2 \\ . & . & . & . \\ . & . & . & . \\ -\ell_{b,N} & -\ell_{t,N} & -1 & \bar{y}_N \end{bmatrix}\begin{bmatrix} \lambda_1 \\ \lambda_2 \\ \lambda_3 \\ \lambda_4 \end{bmatrix} = \begin{bmatrix} 2(\ell_{b,1} - \bar{y}_1\ell_{t,1})X_{b,1} \\ 2(\ell_{b,2} - \bar{y}_2\ell_{t,2})X_{b,2} \\ . \\ . \\ 2(\ell_{b,N} - \bar{y}_N\ell_{t,N})X_{b,N} \end{bmatrix} \quad (22)$$

Equation 21 is a rewriting of the constraints, while eq 22 is the actual solution of the Lagrange minimization. Together they should form a solvable set of equations and unknowns. A solution is consistent with the assumption of equilibrium on the outlet of all trays but has not yet been found. To check how the theory performs, we used linear regression on eq 22. The resulting correlation coefficient and standard errors give an indication of how accurate results of this method can be.

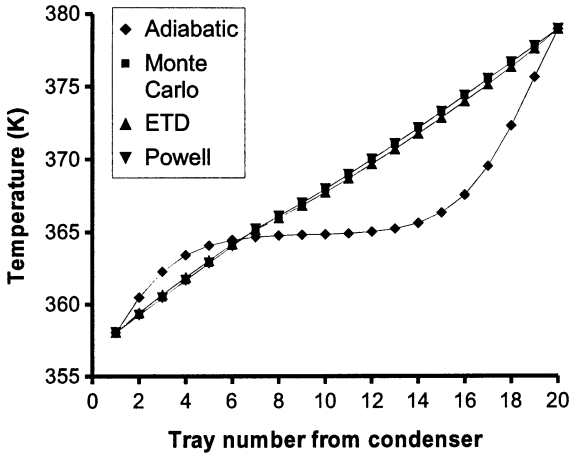

Figure 1. Temperature profiles of column A.

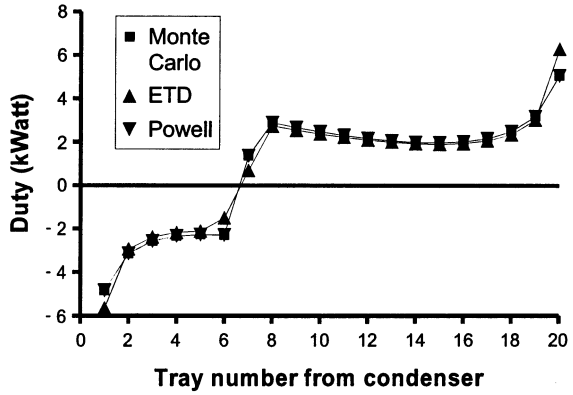

Figure 2. Duty profiles of column A.

Table 3. Total Entropy Production in W/K of the Adiabatic and Diabatic Columns

	adiabatic	ETD	Powell	Monte Carlo
A	2.1687	0.78211	0.77723	0.77692
B	4.0357	(1.4887)	3.3007	3.2977
C	3.0724	0.61202	0.60508	0.60136

7. Results and Discussion

7.1. Minimization Results. The minimum entropy production rates of the columns are calculated from eq 5 (including the contribution of the feed and products), after the ETD, Powell's, and Monte Carlo minimizations are done. The results are given in Table 3. The entropy production rates of the corresponding adiabatic columns are included for comparison.

In all cases, the Monte Carlo method gave the lowest entropy production rates, followed closely by Powell's method. The ETD method gave a lower value for column B, but this result was not physically realizable because it had a negative vapor and liquid flow in the top and bottom of the column. For all columns the reduction in entropy production rate compared to the adiabatic operation was significant. Figures 1, 3, and 5 show the temperature profiles resulting from the ETD, Monte Carlo, and Powell's minimization methods. The temperature profiles of the adiabatic simulation are included for comparison. The corresponding duty profiles

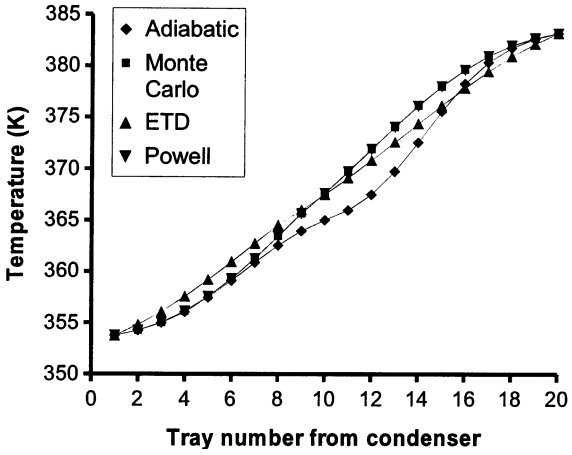

Figure 3. Temperature profiles of column B.

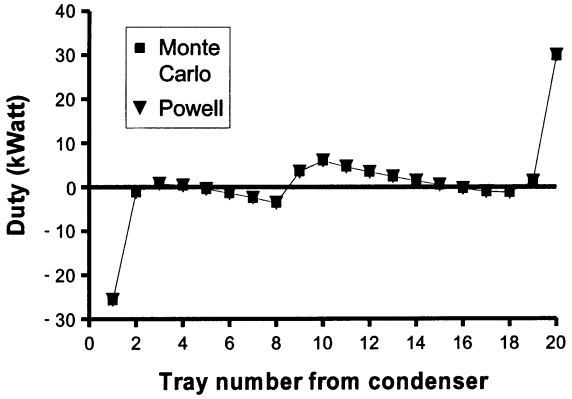

Figure 4. Duty profiles of column B.

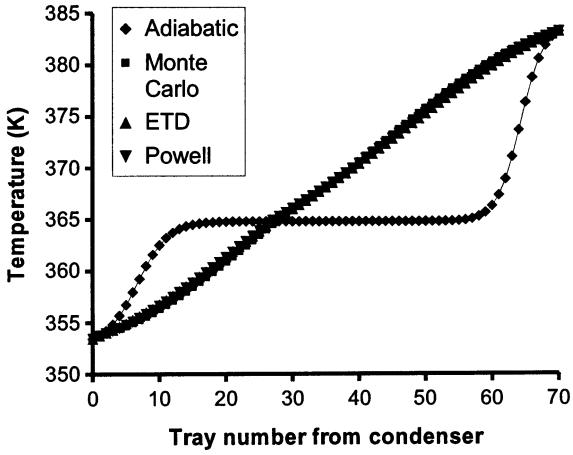

Figure 5. Temperature profiles of column C.

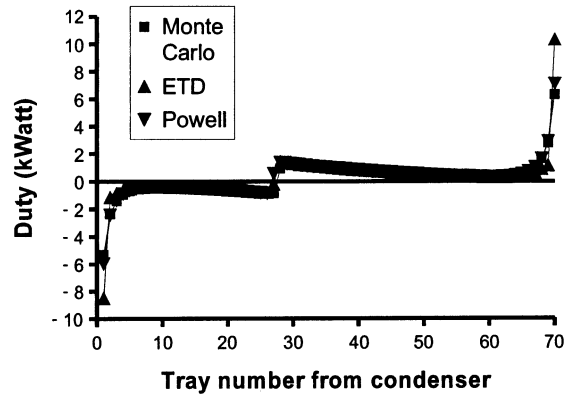

Figure 6. Duty profiles of column C.

of all columns are presented in Figures 2, 4, and 6, which are the answer to the central question posed in the Introduction.

The results of the three minimization methods are nearly indistinguishable for column A, but not for columns B and C. Furthermore, the profiles of the adiabatic columns differ a lot from those of the columns with minimum entropy production. This will be discussed later.

Table 4 presents the results of the application of the Lagrange minimization on irreversible thermodynamics. It consists of the values of the Lagrange multipliers and their standard errors and the total correlation coefficients. All values were calculated using linear regression of eq 22 on the data from the Monte Carlo method. The correlation coefficient and standard errors were best for column A, thereafter C, and finally B.

7.2. Comparison of the Methods. We start with the methods giving the best results: the numerical ones. Table 3 and Figures 1−6 give confidence to both numerical methods because their results essentially agree for all three columns. The results that the total entropy production rate increases by decreasing the number of trays from 70 (C) to 20 (B), or by increasing the purity of the production from 10% (A) to 1% (B), are as expected.

The lower entropy production rate of a diabatic column, compared to that of an adiabatic column, gives the rationale for all minimization methods. We know that neither method guarantees a global minimum. However, the near equality of the results gives us confidence that we have actually obtained the global minimum with both numerical methods. The Monte Carlo algorithm resulted in a slightly lower entropy production rate than Powell's algorithm; see Table 3. This is presumably due to inaccuracies in the estimated gradient obtained by Powell's method. However, the Monte Carlo algorithm took more time to get to the minimum than Powell's algorithm did. The Monte Carlo method gave a steady minimum after several hours, sometimes days, while Powell's method was ready after 1−2 h. In general, for Powell's method, minimum entropy production was obtained after a few N iterations using a relative accuracy of 10^{-9}. In judging the results, it should also be kept in mind that different computers were used. However, the difference in time is reasonable because the Monte Carlo algorithm used most of the computing effort on calculations of temperature profiles that were nonphysical, or that had a higher entropy production rate. We conclude that the results of both numerical methods can be taken as a benchmark for the evaluation of analytical methods.

A singularity problem may arise using Powell's algorithm. The entropy production in eq 5 consists of terms of the form Q_n/T_n, which, in turn, are functions of the liquid and vapor flows V_n and L_n. An explicit representation of the vapor flow above the feed is given by

$$V_n(T_n,T_{n-1}) = \frac{x_b^D - x_{b,n-1}(T_{n-1})}{y_{b,n}(T_n) - x_{b,n-1}(T_{n-1})}D \qquad (23)$$

Analogous expressions exist for the liquid flows and the trays below the feed. Equation 23 has a singularity; the flow becomes infinite for $y_{b,n} = x_{b,n-1}$. This leads to an undesired instability of the minimization algorithm: At the beginning of a line minimization along a

Table 4. Lagrange Multipliers of the Minimum Entropy Producing Columns Calculated with Linear Regression

	referring to	A	B	C	units
λ_1	l_1	-0.213 ± 0.018	-0.167 ± 0.021	0.0775 ± 0.0055	J/mol·K
λ_2	l_2	0.917 ± 0.051	3.65 ± 0.48	-0.712 ± 0.035	J/mol·K
λ_3	intercept	-0.0462 ± 0.0039	-0.123 ± 0.033	0.0276 ± 0.0022	mol/s
λ_4	$\bar{y}_n$	0.0277 ± 0.0018	0.0256 ± 0.0033	-0.00721 ± 0.00026	mol/s
R^2		0.995	0.966	0.983	

particular search direction, the minimum needs to be bracketed. Otherwise, the one-dimensional minimization routine may jump over this singularity and lead to a nonphysical result, e.g., a large negative value for the entropy production.

The method of ETD permits a direct comparison with the numerical methods from the data in Table 3 and Figures 1−6. It is observed that ETD predicted column A better than columns B and C. The maximum deviations with the Monte Carlo benchmark results in predicted temperatures were 0.40 K on tray 15 in column A, 1.87 K on tray 15 in column B, and 0.53 K on tray 56 in column C. The duty profile of ETD is not given for column B in Figure 4 because the solution was nonphysical. Specifically, it had extremely high duties with opposite signs at both ends of the column. As a consequence, it gave (impossible) negative liquid flows on tray 1 (−2.3 mol/s) and 19 (−1.46 mol/s) and negative vapor flows on tray 2 (−1.84 mol/s) and 20 (−1.96 mol/s). This is due to the already mentioned limitation of the ETD method that the tray−tray separation stay small as discussed in connection with eq 16. Column B does not have enough trays for the required thermodynamic distance. For columns of length comparable to what would currently be used in an industrial implementation (like column B), condition (16) is invariably violated. This is why columns A and C, but not B, are well predicted by this method. In conclusion, ETD gives good results for columns with a large number of trays and/or low purities of which the assumption of equilibrium on each tray is valid. However, once a low number of trays and/or high-purity products or nonequilibrium modeling are demanded, it loses its reliability.

Both objective functions, the entropy balance in eqs 5 and 17 from irreversible thermodynamics, describe, in principle, the same column. Their approaches and assumptions differ, however. We have chosen previously the results of the numerical methods that use eq 5 as a benchmark. The correlation coefficients and standard errors from Table 4 give, therefore, an indication of how accurate the method, using Lagrange minimization on eq 17 with the constraints in eq 20, describes the benchmark results. De Koeijer and Kjelstrup[2] give arguments and results for the correctness of the Lagrange minimization with the constraints in eq 20. So, the correlation coefficients and standard errors become a measure of the accuracy of eq 17. The near-unity correlation coefficient for column A can be interpreted by eq 17 as being a good approximation of eq 5. The correlation coefficient for column B is 0.966. This means that eq 17 is a poorer approximation of eq 5 for column B than for A. Inaccurate (and possibly nonphysical) solutions may show up for column B by solving eqs 21 and 22. The results for column C are better than those for column B but not as good as those for column A. Out of the three columns here and two earlier ones,[2] four columns have had correlation coefficients better than 0.98 for this method. The lower correlation coefficients are observed for the columns with high purities and/or hard separation. So, we can say that the assumptions behind eq 17 are not valid for columns operating with these conditions.

The Lagrange minimization with irreversible thermodynamics does not provide (yet) an actual solution, but it has a potential for further development. It gives a systematic way of modeling nonequilibrium phenomena and does not necessarily depend on the assumption of equilibrium on the outlet of all trays. Wesselingh[21] argues even that this equilibrium assumption leads to results that have no connection to real distillation columns. In this perspective, these results can be considered as a base for further work.

There are several differences between the two analytical methods. The first method, ETD, is based on a lowest order asymptotic analysis of the path over the equilibrium surface. The second method with the Lagrange minimization uses irreversible thermodynamics. The objective function, the entropy production rate, is expressed differently. The ETD method uses the total entropy balance of the system. Irreversible thermodynamics uses the sum of flux−force products of the processes that take place. However, their differences have not really been tested here, because the assumption of equilibrium on each tray has been used to find both objective functions. The accuracy of the methods depends on what type of information is needed. The ETD method uses information about equilibrium states, while the second method requires a model of the (nonequilibrium) processes in terms of fluxes, forces, and phenomenological coefficients. The ETD method can then only be accurate if the column operates close to equilibrium and if it has a relatively high number of trays. It has not been tested yet how far from equilibrium the ETD method still predicts accurately. The accuracy of the second method depends on how good that particular model describes reality. When these differences are related to the present work, the ETD method does not describe column B accurately because of the relatively low number of trays, while Lagrange minimization and irreversible thermodynamics fail for column B because of an inaccurate model.

7.3. Diabatic versus Adiabatic Columns. Finally we discuss in more depth the common purpose of the minimization methods: minimizing entropy production rate by adding heat exchangers on each tray. The McCabe−Thiele diagram of diabatic operation with minimum entropy production is given for column A in Figure 7. Figure 8 shows the McCabe−Thiele diagram of the corresponding adiabatic column A. The operating line is more parallel to the equilibrium line in a diabatic column than in an adiabatic column. This behavior was observed for a rectifying column.[22] Sauar et al.[22] found this to be consistent with equipartition of forces for larger parts of the column. The diagram in Figure 8 indicates already that there is room for improvement in the adiabatic column because the trays around the feed do not perform a reasonable separation; i.e., this adiabatic column is badly designed from a second law perspective.

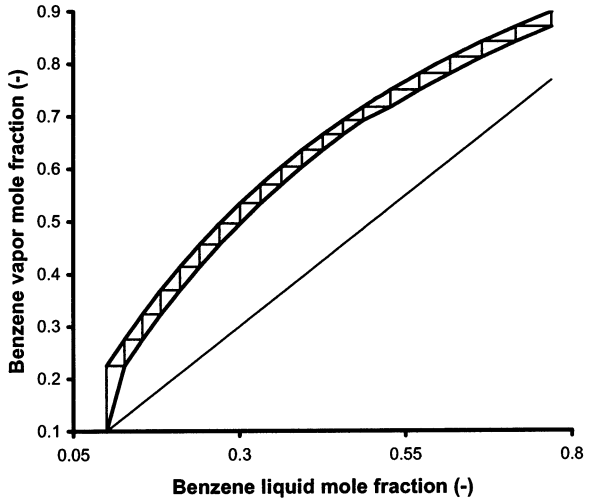

Figure 7. McCabe−Thiele diagram of diabatic column A with a minimum entropy production rate.

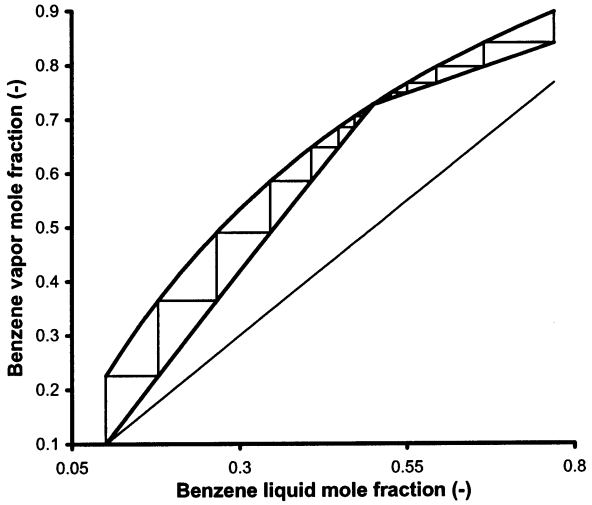

Figure 8. McCabe−Thiele diagram of adiabatic column A.

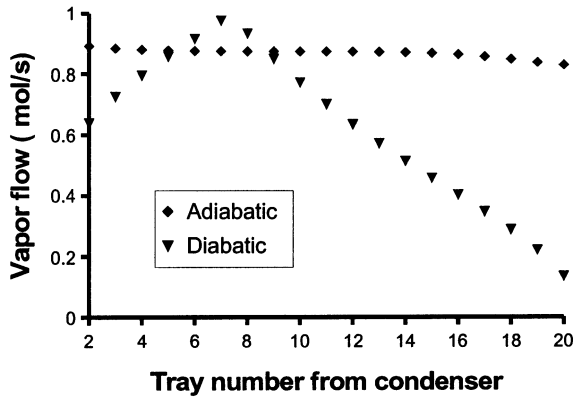

Figure 9. Vapor flow profile of column A.

To illustrate the difference between adiabatic and diabatic columns further, we give the vapor and liquid flow profiles of column A in Figures 9 and 10. The discontinuity in the liquid profiles is due to the feed, which is a liquid at its boiling point. This location of the feed tray is moved from tray 9 in the adiabatic to tray 7 in the diabatic column; i.e., the stripping section is enlarged. We see that the vapor flow is rather constant for the adiabatic column. This allows the normal column design with constant diameter because the diameter is roughly proportional to the vapor flow.

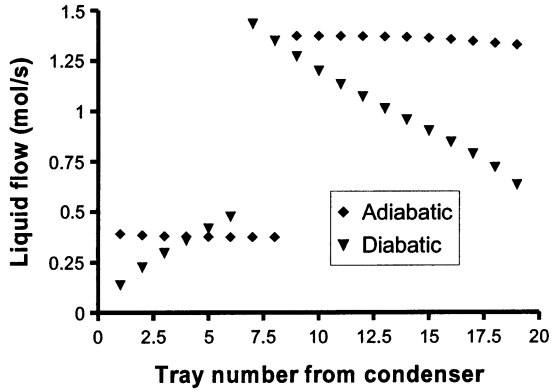

Figure 10. Liquid profile of column A.

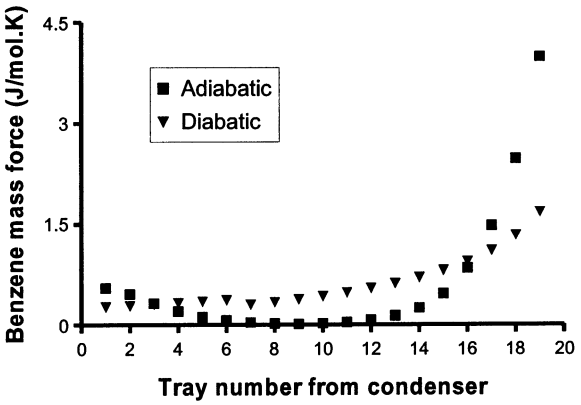

Figure 11. Benzene mass force profile of adiabatic and diabatic column A.

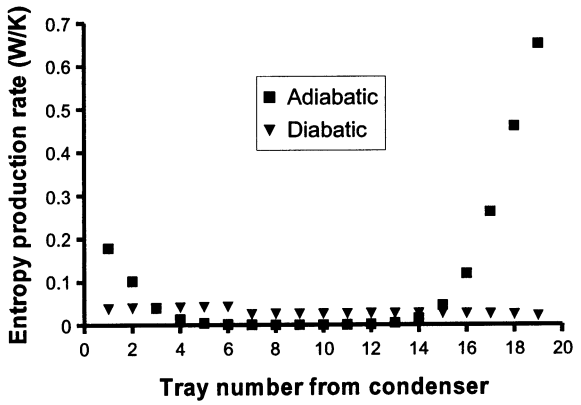

Figure 12. Entropy production rate calculated with eq 17 of adiabatic and diabatic column A.

The vapor flow in a diabatic column is not constant. Design of a column that allows this behavior of the vapor flow is clearly a challenge for chemical engineers. A constant diameter may increase the risk for uneven pressure drops, flooding, or dry-up. On the other side, a column with a varying diameter is more expensive.

Neither the entropy production rate[9] nor the driving force for mass transport[23] is constant in the diabatic column A with minimum entropy production rate. Figures 11 and 12 show the benzene driving force from eq 18 and the entropy production rate from eq 17 as a function of the tray number counted from the condenser. The entropy production varies by a factor of 2 over the diabatic column. The force varies even more. A constant force through the column is also not expected, given the nature of the constraints in eq 20.[24] Figures 11 and 12 do show, however, that separation work is moved from

the top and bottom ends to the middle part as a consequence of the minimization and that the variation in the force as well as in the entropy production rate is more uniform in the diabatic than in the adiabatic column.

8. Conclusions

Two analytical and two numerical methods for minimizing the entropy production rate in diabatic binary distillation are compared. The two numerical methods, which are based on Powell's method and a Monte Carlo algorithm, give similar results and the lowest entropy production rates. The analytical method of ETD gives results that are in agreement with the numerical methods for two columns with a large number of trays and/or low-purity products. However, for a column with high-purity products and a low number of trays, it gives a nonphysical solution. The analytical method based on applying Lagrange minimization on irreversible thermodynamics gives no direct result, but its solution is in agreement with the numerically obtained minima for the same two columns as ETD, according to a linear regression analysis. Lagrange minimization also describes inaccurately the results for column B, the same column for which ETD gives a nonphysical solution. More work is clearly needed to make the analytical methods useful. In the meantime, the numerical methods may serve the practical purpose of optimization.

Only the entropy production rates due to tray processes are taken into account in the above calculations. The contribution to the entropy production rate from the heat exchangers is not considered. Such contributions will change the relative gain from making the column diabatic.

Even though the analytical methods presented still have their limitations, it is important to note that there are now highly effective numerical methods available for the design and analysis of diabatic distillation columns. The second law gains available from such columns worldwide are very significant, especially in an environment where the CO_2 production should be reduced to levels well below current values. We believe that the methods presented here, especially the analytical ones, offer ample opportunities for further research in this field.

Acknowledgment

The Telluride Research Center is thanked for hosting the workshop at which this cooperation was initiated. The Research Council of Norway is thanked for a grant to G.d.K.

Symbols

B = bottom (mol/s)
C_σ = constant-pressure coexistence heat capacity (J/K)
D = distillate (mol/s)
F = feed (mol/s)
H = enthalpy (J/mol)
I = value of the constraint (mol/s or J/mol·K)
J = flow through the phase boundary (mol/s or J/s)
L = liquid flow (mol/s)
$\mathrm{d}\ell$ = thermodynamic length ($\sqrt{\mathrm{J/K}}$)
ℓ = phenomenological coefficient (mol²·K/s·J)
M = number of search directions in Powell's algorithm
N = number of trays
Q = duty (J/s)
R = gas constant (J/mol·K)
R^2 = correlation coefficient
S = entropy (J/mol·K)
T = temperature (K)
Z = extensive variables of the system (various)
$\tilde{\mathbf{T}}$ = temperature profile (K)
$\tilde{\mathbf{u}}$ = search direction (K)
V = vapor flow (mol/s)
X = force (J/mol·K or 1/K)
x = liquid mole fraction
y = vapor mole fraction
$\bar{y}$ = averaged Gibbs−Duhem vapor mole fraction ratio[2]
$\mathrm{d}S^{\mathrm{irr}}/\mathrm{d}t$ = entropy production rate (J/s·K)
λ = Lagrange multiplier (mol/s or J/mol·K)
Σ = largest decrease in Powell's algorithm (J/s·K)
ξ = definition introduced in eq 7
ω = nonideality parameter

Superscripts and Subscripts

B = bottom
b = benzene
boil = boiling
D = distillate
E = extrapolated point in eq 7
i = component number i
j = search direction index in Powell's algorithm
L = liquid
n = tray number n
N = total number of trays
t = toluene
V = vapor

Literature Cited

(1) Andresen, B.; Salamon, P. Optimal distillation calculated by thermodynamic geometry. *Entropie* **2000**, *36*, 4.

(2) De Koeijer, G.; Kjelstrup, S. Minimizing entropy production in binary tray distillation. *Int. J. Appl. Thermodyn.* **2000**, *3* (3), 105.

(3) Fonyo, Z. Thermodynamic analysis of rectification. I. Reversible model of rectification. *Int. Chem. Eng.* **1974**, *14* (1), 18.

(4) Fonyo, Z. Thermodynamic analysis of rectification. II. Finite cascade models. *Int. Chem. Eng.* **1974**, *14* (2), 203.

(5) Rivero, R. L'Analyse d'Exergie: Application *à* la Distillation Diabatique et aux Pompes *à* Chaleur *à* Absorption. Ph.D. Dissertation, Institut National Polytechnique de Lorraine, Nancy, France, 1993.

(6) Le Goff, P.; Cachot, T.; Rivero, R. Exergy analysis of distillation processes. *Chem. Eng. Technol.* **1996**, *19*, 478.

(7) Agrawal, R.; Fidkowski, Z. On the use of intermediate reboilers in the rectifying section and condensers in the stripping section of a distillation column. *Ind. Eng. Chem. Res.* **1996**, *35* (8), 2801.

(8) Rivero, R. Exergy simulation an optimization of adiabatic and diabatic binary distillation. *Energy* **2001**, *26*, 561.

(9) Tondeur, D.; Kvaalen, E. Equipartition of entropy production. An optimality criterion for transfer and separation processes. *Ind. Eng. Chem. Res.* **1987**, *26* (1), 50.

(10) Kauchali, S.; McGregor, C.; Hildebrandt, D. Binary distillation re-visited using the attainable region theory. *Comput. Chem. Eng.* **2000**, *24*, 231.

(11) Press, W. H.; Vetterling, W. T.; Teukolsky, S. A.; Flannery, B. P. *Numerical Recipes in C*; Cambridge University Press: Cambridge, U.K., 1992.

(12) Schaller, M.; Hoffmann, K. H.; Siragusa, G.; Salamon, P.; Andresen, B. Numerically optimized performance of diabatic distillation columns. *Comput. Chem. Eng.* **2001**, *25* (11−12), 1537.

(13) Pitzer, K.; Brewer, L. *Thermodynamics*; McGraw-Hill: New York, 1961.

(14) Førland, K. S.; Førland, T.; Kjelstrup, S. *Irreversible Thermodynamics. Theory and Application*, 3rd ed.; Tapir: Trondheim, Norway, 2001.

(15) Salamon, P.; Nulton, J. The geometry of separation processes: A horse-carrot theorem for steady flow systems. *Europhys. Lett.* **1998**, *42* (5), 571.

(16) Nulton, J.; Salamon, P.; Andresen, B.; Anmin, Q. Quasistatic processes as step equilibrations. *J. Chem. Phys.* **1985**, *83* (1), 334.

(17) Ruppeiner, G. Riemannian geometry in thermodynamic fluctuation theory. *Rev. Mod. Phys.* **1995**, *67* (3), 605.

(18) Nulton, J. D.; Salamon, P. Optimality in multi-stage operations with asymptotically vanishing cost. *J. Nonequilib. Thermodyn.* **2002**, submitted for publication.

(19) De Koeijer, G.; Kjelstrup, S.; Van der Kooi, H. J.; Gross, B.; Knoche, K. F.; Andersen, T. Positioning heat exchangers in binary tray distillation using isoforce operation. *Energy Convers. Manage.* **2002**, *43* (9−12), 1571.

(20) Kjelstrup-Ratkje, S.; Sauar, E.; Hansen, E.; Lien, K.; Hafskjold, B. Analysis of entropy production rates for design of distillation columns. *Ind. Eng. Chem. Res.* **2001**, *34* (9), 3001.

(21) Wesselingh, J. A. Nonequilibrium modelling of distillation. *Chem. Eng. Res. Des. (Trans. Inst. Chem. Eng.)* **1997**, *75A*, 529.

(22) Sauar, E.; Rivero, R.; Kjelstrup, S.; Lien, K. M. Diabatic column optimization compared to isoforce columns. *Energy Convers. Manage.* **1997**, *38* (15−17), 1777.

(23) Sauar, E.; Kjelstrup, S.; Lien, K. M. Equipartition of forces: A new principle for process design and operation. *Ind. Eng. Chem. Res.* **1996**, *35* (11), 4147.

(24) Bedeaux, D.; Standaert, F.; Hemmes, K.; Kjelstrup, S. Optimization of processes by equipartition. *J. Nonequilib. Thermodyn.* **1999**, *24*, 242.

Received for review October 24, 2001
Revised manuscript received August 22, 2002
Accepted August 28, 2002

IE010872P